Luminescence quenching studies of CeF_3 and $CeF_3 - LaF_3$ by means of nanosecond time-resolved VUV spectroscopy

1996 J. Phys.: Condens. Matter 8 497

(http://iopscience.iop.org/0953-8984/8/4/014)

J. Phys.: Condens. Matter **8** (1996) 497–504. Printed in the UK

Luminescence quenching studies of CeF_3 and CeF_3–LaF_3 by means of nanosecond time-resolved VUV spectroscopy

M A Terekhin†‡, I A Kamenskikh§, V N Makhov‖, V A Kozlov‖, I H Munro‡, D A Shaw‡, C M Gregory‡ and M A Hayes‡

† 'Kurchatov Institute' Russian Research Centre, Moscow 123182, Russia
‡ Daresbury Laboratory, Warrington, Cheshire WA4 4AD, UK
§ Moscow State University, Moscow 117234, Russia
‖ Lebedev Physical Institute, Moscow 117924, Russia

Received 2 May 1995, in final form 23 November 1995

Abstract. The quenching mechanisms for fast luminescence in CeF_3 and CeF_3–LaF_3 crystals have been studied by means of time-resolved VUV spectroscopy using synchrotron radiation. The luminescence decay of these crystals reveals at least three mechanisms of quenching: the first one, conventional for the VUV region, where the radiation penetration depth is very small ~10 nm, results from surface losses; the second one is due to the energy transfer to defect centres in the bulk of the crystal (very pronounced in CeF_3–LaF_3) and the third one, the least studied, is attributed to the interaction of closely spaced electron excitations (secondary-electron excitation quenching). The temperature and energy dependencies of the decay kinetics clearly indicate that the last quenching mechanism comes into play above the energy corresponding to the threshold for the creation of secondary-electron excitations.

1. Introduction

For the successful use and manufacture of fast scintillator materials which have wide practical applications both in high-energy physics and medicine [1, 2] the understanding of fundamental processes responsible for quenching of the luminescence is crucially important. In the wide-band-gap scintillator crystals CeF_3 and BaF_2, an unusual type of quenching of prompt intrinsic luminescence under moderate-intensity VUV excitation has been observed recently [3–5]. It is assumed that the effect is associated with a non-radiative energy transfer between the VUV excited luminescence centre (the $(Ce^{3+})^*$ or 5p Ba^{3+} core hole) and the nearest electron excitations created by the same absorption process [6]. This mechanism was advanced as an explanation of quenching seen in the initial stage of luminescence decay after x-ray excitation in some nanosecond scintillators [7, 8]. The closely spaced interacting electron excitations are formed by inelastic scattering of primary photoelectrons and Auger relaxation of core photoholes created by the absorption of the VUV photon. Since the mean free path of the photoelectron excited by the VUV photon with energy $E > 2E_g$ in respect of electron–electron inelastic scattering has a value of about 0.5 nm [9], we expect that even after the process of the thermalization the distance between secondary-electron excitations could be comparable with the radius R_0 of dipole–dipole energy transfer with the rate $W \sim \tau^{-1}(R_0/R)^6$ [10], where τ is the lifetime of the electron excitations. For instance, in the case of resonance transfer from the 5p Ba^{3+} core hole to the Ce^{3+} ion in barium fluoride, R_0 is about 1.2 nm [11].

0953-8984/96/040497+08$19.50

This effect, which displays the fundamental process of electron–electron inelastic scattering in crystalline materials, is believed to be important for many fast luminescent crystals and must be studied further. As the minimum threshold for electron–electron scattering is about $2E_g$, the use of VUV excitation allows one to follow how this mechanism switches on. In this region the absorption coefficient is very high, i.e. the radiation penetration depth is very small (less than 10 nm) and near-surface luminescence quenching should be taken into account [12].

The aim of this research is to extend our investigations into the effects of luminescence quenching in pure CeF_3 and mixed CeF_3–LaF_3(10%) crystals, paying special attention to non-radiative energy transfer between the luminescent centre Ce^{3+} and the nearest secondary-electron excitations.

2. Experimental procedure

CeF_3–LaF_3 crystals with a concentration of 10% LaF_3 were grown by the Stockbarger–Bridgeman method in a fluorine atmosphere. Crystals were cleaved just prior to their installation into the cryostat. The CeF_3 sample was a high-purity powder with a total impurity concentration of less than 20 ppm.

Synchrotron radiation from the SRS (Daresbury Laboratory) was used as a light source. The excitation and emission spectra were measured in multibunch operation while luminescence decay curves were derived in single-bunch mode of the SRS on station 3.1, using a 1 m Seya–Namioka monochromator covering the VUV photon range 5–35 eV [13]. The luminescence was observed via interference filters and a visible/UV monochromator (SPEX Minimate) with a resolution of 5 nm. Low-temperature measurements were performed using an UHV continuous-flow helium cryostat (Oxford instruments) with temperature controller (model ITC4). The residual pressure in the sample chamber during collection of experimental data was 2×10^{-7} Pa.

Luminescence decay time studies were made using the single-photon coincidence method [14]. Decay curves were reasonably well fitted by a sum of three exponentials using the computer code FLUOR [15]. The derived decay times fall into three ranges: $\tau_1 \sim$ 2–4 ns for the shortest one, $\tau_2 \sim$ 12–20 ns and $\tau_3 \sim$ 40–60 ns. The large range of parameters is caused by a complicated non-exponential decay law due to the combination of different quenching mechanisms. The emission decay of 'perturbed' Ce^{3+} was characterized by a rise time in agreement with the model of luminescence in a CeF_3-like system [16–22].

3. Experimental results and discussion

3.1. Emission and excitation spectra

Figure 1 presents the luminescence spectrum of CeF_3–LaF_3 at 300 K and 20 K excited with 8.4 eV photons. We can see four main features at wavelengths of 290, 310, 325, and 390 nm. The first two bands correspond to emission from the 'normal' (unperturbed) Ce^{3+} in the cation position [3, 16, 19, 23] while the latter two are associated with Ce^{3+} perturbed by some impurity or intrinsic defects, e.g. O^{2-} or (and) an anion vacancy in its first coordination sphere [18–21]. The same situation has been observed in pure cerium fluoride and CeF_3 activated by the divalent cations Ca^{2+}, Cd^{2+}, Ba^{2+} where the broad emission band of 'perturbed' Ce^{3+} luminescence was in the spectral region 320–380 nm [3, 20, 21]. Luminescence studies of pure CeF_3 powder have not shown the perturbed Ce^{3+} emission.

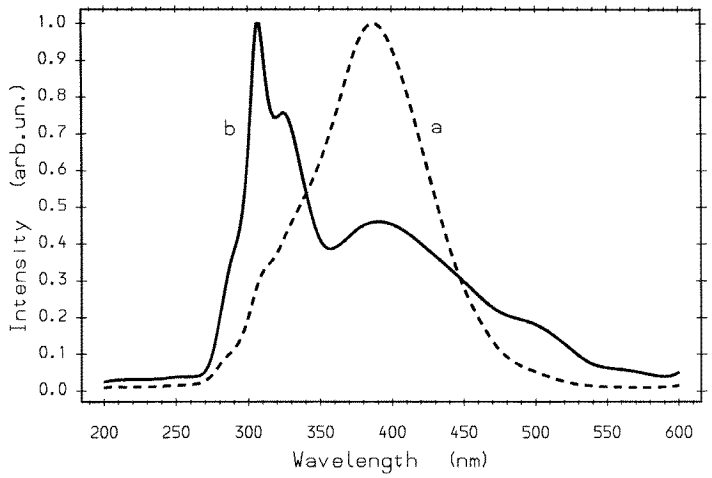

Figure 1. The emission spectrum of CeF_3–LaF_3(10%) at (a) 300 and (b) 20 K. The excitation energy $E_{ex} = 8.4$ eV.

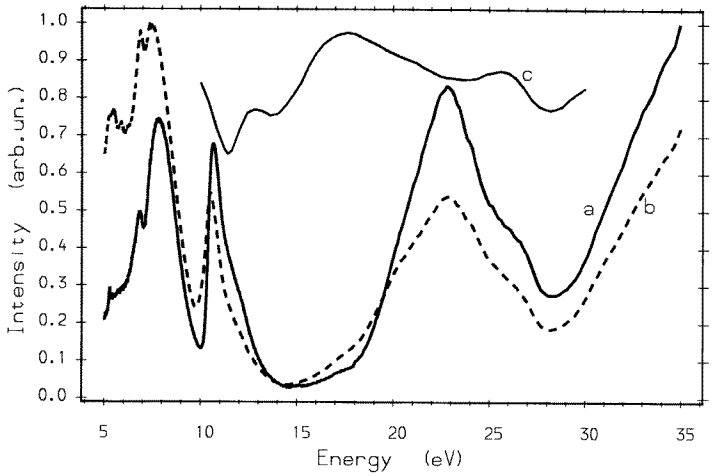

Figure 2. The luminescence excitation spectra of CeF_3–LaF_3(10%) for (a) normal Ce^{3+} (290 nm) and (b) perturbed Ce^{3+} (390 nm) at 300 K; (c) the absorptivity spectrum $(1 - r)$ for CeF_3, where r is the reflectivity measured in [26].

Figure 2 shows the excitation spectrum of the normal and perturbed emission bands at 300 K. The spectra are very similar to each other and that of pure CeF_3 measured previously [3, 4, 24]. The structure in the region 5–7 eV corresponds to the excitation 4f $\rightarrow$ 5d while the wide band at 8.4 eV can be attributed to the 4f $\rightarrow$ 6s transitions of Ce^{3+} or charge transfer of 2p $F^- \rightarrow$ 6s Ce^{3+} in CeF_3 [18, 25]. In the energy region 10–35 eV we observed two wide bands, at 10 –15 eV and 20–27 eV, and an increase of the luminescence efficiency at energies above 30 eV. The latter region corresponds to the electronic transitions with strong absorption from the (2p F^-) valence band and 5p levels of lanthanides to the conduction band [26]. The wide band with a maximum at 10.6 eV is formed by increasing of luminescence efficiency near the edge of fundamental absorption $E_g \sim 10$ eV and the strong

decrease above E_g due to the energy dependence of the electron–hole binding probability, which controls the VUV excitation process in CeF_3 [4]. The second band with a maximum at 22.9 eV is believed to be associated with rising of emission intensity near the threshold of the creation of secondary-electron excitations $\sim 2E_g \sim 20$ eV and the pronounced dropping above $2E_g$ due to both the energy dependence of electron–hole binding probability and secondary-electron quenching effects which will be discussed further. The shoulders at 12 eV, 17 eV and 26 eV in the luminescence excitation spectra are caused by crystal absorptivity $(1 - r)$ [12], where r is the reflectance of CeF_3 in the VUV region [26]. It is clearly seen from figure 2 that the above-mentioned peculiarities in the excitation spectra (curves a, b) correspond to the maxima in $1 - r$ (curve c).

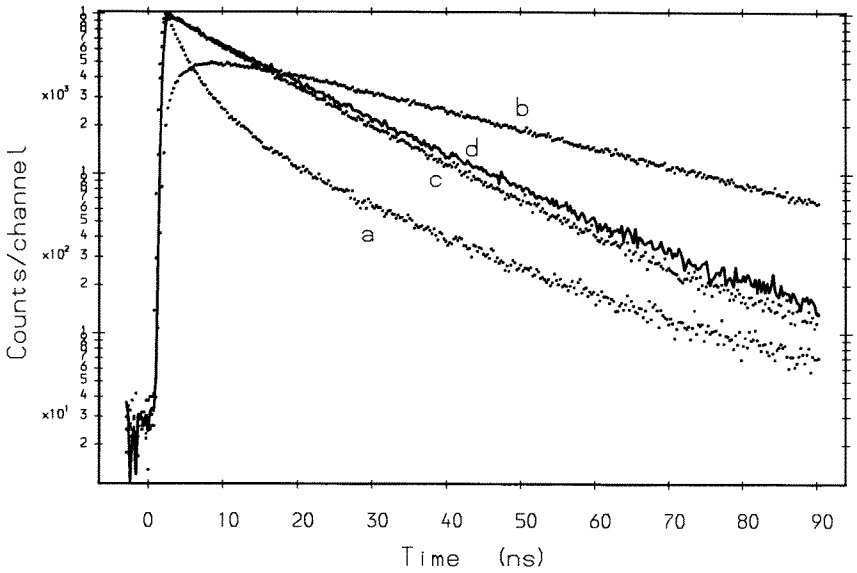

Figure 3. Decay curves for $E_{ex} = 8.4$ eV. (a) Normal Ce^{3+} emission of CeF_3–LaF_3(10%), $T = 300$ K. (b) Perturbed Ce^{3+} emission of CeF_3–LaF_3(10%), $T = 300$ K. (c) Normal Ce^{3+} emission of pure CeF_3, $T = 300$ K. (d) Normal Ce^{3+} emission of pure CeF_3, $T = 20$ K.

3.2. Decay curves

3.2.1. Temperature dependence. Figure 3 presents the decay curves for normal Ce^{3+} emission for both compounds and perturbed Ce^{3+} luminescence in CeF_3–LaF_3 following excitation in the region of the $4f \rightarrow 5d, 6s$ transitions. Figure 4 demonstrates the temperature dependences in the range 20–300 K for decay curves for the normal Ce^{3+} emission in CeF_3–LaF_3 crystals and their asymptotic approach to the decay curve of pure CeF_3 at 20 K (the top curve in figure 4). The deviation from one exponential decay law for CeF_3–LaF_3 is supposed to be mainly associated with non-radiative resonance energy transfer from normal $(Ce^{3+})^*$ to perturbed Ce^{3+} [18, 20, 21]. For pure CeF_3 the decay time at 5.6 eV and 8.4 eV slightly decreases with a rise of temperature across the range 20–300 K, without any significant changes (figure 3, curves c, d). The effect is less than that at 12 eV (figure 6, curves a, b—below) and could be successfully explained in terms of surface losses which will be discussed below.

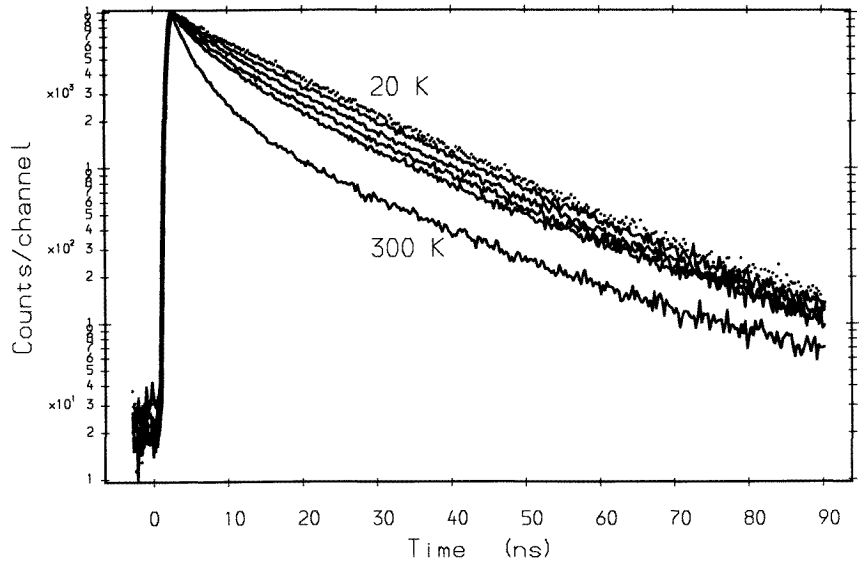

Figure 4. Decay curves for normal Ce^{3+} emission for $E_{ex} = 8.4$ eV in CeF_3–LaF_3(10%) at $T = 300$, 200, 150, 100 and 50 K. The lifetime increases steadily from 300 (the lowest) to 50 K (upper) curve. The top curve is CeF_3 at $T = 20$ K.

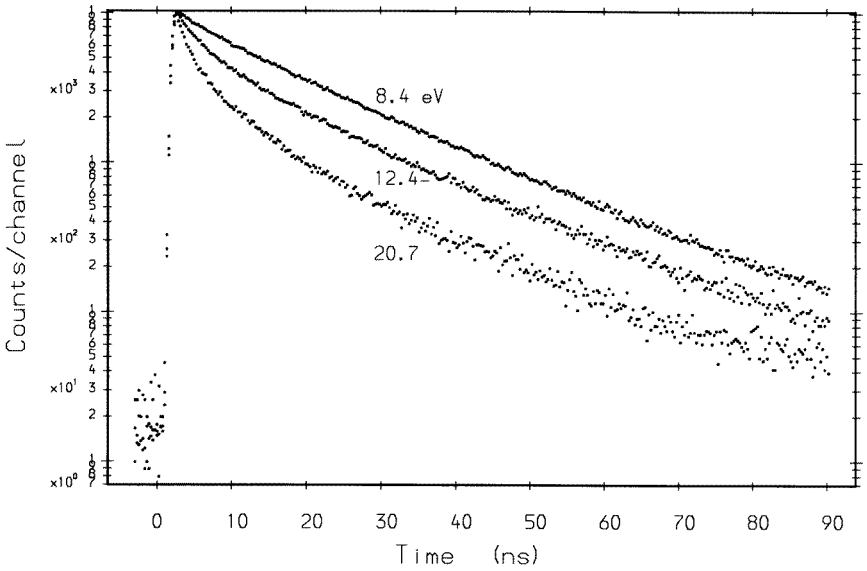

Figure 5. Decay curves for normal Ce^{3+} emission from CeF_3–LaF_3(10%) at 20 K. E_{ex} = 8.4 (upper curve), 12.4 (centre curve) and 20.7 eV (lower curve).

3.2.2. The excitation energy dependence. In the excitation region, corresponding to the Ce^{3+} absorption from 5 to 10 eV, the radiation penetration depth is rather high and the surface losses are small. However, in the region of transitions involving the fluorine states

($E > 10$ eV [26]) the surface quenching is expected to be higher. Both of these cases are illustrated in figure 5 for CeF_3–LaF_3 at low temperature, when the non-radiative energy transfer between normal and perturbed Ce^{3+} could be ignored. It is interesting that at lower energy, 12.4 eV (figure 5), the shortening of the decay is not so strong in comparison with that at 20.7 eV, despite a decrease in the absorption coefficient from 1.6×10^6 to 1.2×10^6 cm^{-1}. The changes in absorption coefficient were estimated by the Kramers–Kronig analysis of the reflectivity spectrum for s-polarized light of crystal CeF_3 measured in [26]. Therefore there must be an additional quenching mechanism if neither surface losses nor resonance energy transfer to perturbed Ce^{3+} centres could decrease the decay time so strongly. For CeF_3, since the excitation energy is 16 eV as a result of inelastic scattering of the fast photoelectron by Ce^{3+} ions (i.e. impact excitation of Ce^{3+} [24, 27]) and, beginning from $2E_g \sim 20$ eV, by the electrons of the (2p F^-) valence band, closely spaced secondary-electron excitations are created [3, 4]. As the luminescence quenching manifests itself in shortening of decay curves without any changes in rise time, and taking into consideration the results of [19], we have come to the conclusion that the additional mechanism of quenching revealed at 20.7 eV is a non-radiative energy transfer between the normal excited Ce^{3+} and the nearest secondary-electron excitation.

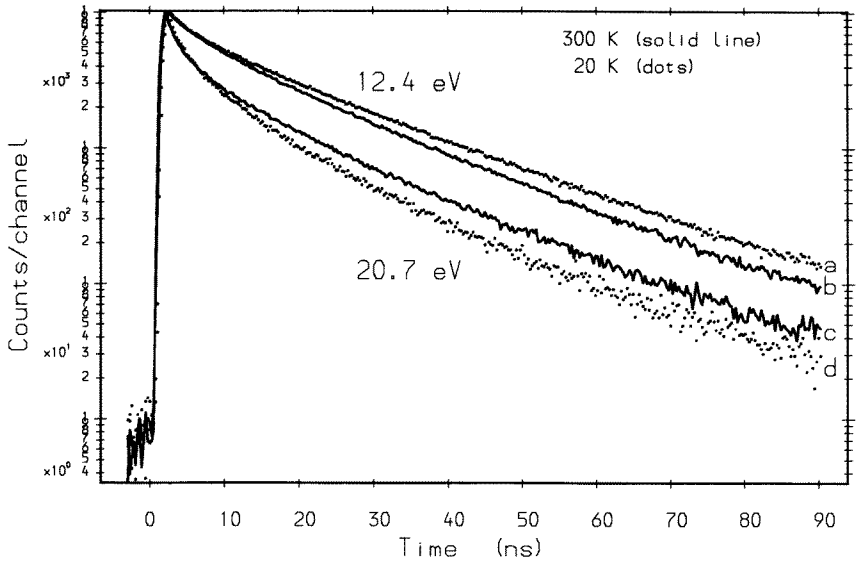

Figure 6. Decay curves for normal Ce^{3+} emission from CeF_3. (a) $E_{ex} = 12.4$ eV, $T = 20$ K. (b) $E_{ex} = 12.4$ eV, $T = 300$ K. (c) $E_{ex} = 20.7$ eV, $T = 300$ K. (d) $E_{ex} = 20.7$ eV, $T = 20$ K.

The assumption that the dominant mechanism of quenching changes is confirmed by figure 6, where the temperature dependence of decay curves in CeF_3 with excitation above and below the threshold energy for the creation of secondary-electron excitations is presented. The effect of temperature on the decay curves is reversed in these two cases. For an excitation energy at 12.4 eV (figure 6, curves a, b), when the surface losses are assumed to be dominant, the luminescence quenching is greater at room temperature than at 20 K. Two mechanisms of the surface quenching are postulated [12]: namely, resonance and (or) diffusion energy transfer from electron excitations to the quenching centres, the concentration of which is much larger near to the surface than in the volume of

a crystal. Thus we can conclude that the faster decay of the luminescence with temperature, at an excitation of 12.4 eV, is associated with the increasing diffusion mobility of electron excitations. The reverse effect with temperature is observed at an excitation energy of 20.7 eV (figure 6, curves c, d) when the secondary-electron excitation at a distance $\sim R_0$ from $(Ce^{3+})^*$ could be created such that secondary-electron excitation quenching should take place. In the latter case the rise of electron excitation mobility with temperature will increase the mean distance R between $(Ce^{3+})^*$ and electron excitation created in the same absorption process which reduces the probability of secondary-electron excitation quenching.

4. Conclusions

The quenching due to the interaction with geminate secondary-electron excitations has been identified in pure CeF_3 and CeF_3–LaF_3 crystals. In these fast scintillators the Ce^{3+} luminescence is quenched by the nearest electronic excitation (excited Ce^{3+}, electrons or holes etc) created by the same absorption process, as a result of inelastic scattering of the hot photoelectron (or Auger decay of core hole). It has been shown that the secondary-electron excitation quenching effect is found once the excitation energy is sufficient for the creation of secondary-electron excitations and obviously starts with the threshold of the electron multiplication in the scintillator. It has been revealed for pure CeF_3 that when the quenching by secondary excitation is expected to take a role (above 16 eV) the temperature dependence of the decay curves is opposite to that in the region 5–13 eV where the near-surface losses are dominant. The magnitude of secondary-electron excitation quenching seems to decrease with the mobility of the electronic excitations.

The surface losses are traditionally assumed to provide the main mechanism for luminescence quenching with VUV excitation but this work demonstrates that such is not always the case. For CeF_3 and CeF_3–LaF_3 at an excitation energy of 20.7 eV, the secondary-electron excitation quenching effect is more significant.

The understanding of this quenching effect is extremely important for practical scintillator applications, particularly those where the scintillator detectors are operated in the VUV and soft x-ray regions where the mean free path of photoelectron and secondary-electron excitations is very small.

Acknowledgments

The experiments were carried out at the CLRC Synchrotron Radiation Division, Daresbury Laboratory. The work was supported by the Science and Engineering Research Council of the UK in the framework of the UK–Russian Collaboration on Synchrotron Radiation. The authors would like to thank Dr A N Vasil'ev for valuable discussions and Dr T V Uvarova for the growth of the CeF_3–LaF_3 crystals.

References

[1] Anderson S *et al* (82 authors) 1993 *Nucl. Instrum. Methods* A **332** 373
[2] Lecoq P and Schussler M 1992 *Nucl. Instrum. Methods* A **299** 51
[3] Kamenskikh I A, MacDonald M A, Makhov V N, Munro I H, Mikhailin V V and Terekhin M A 1994 *Nucl. Instrum. Methods* A **348** 542
[4] Pedrini C, Belsky A N, Vasil'ev A N, Bouttet D, Dujardin C, Moine B, Martin P and Weber M J 1994 *Proc. Mater. Res. Soc. Symp.* **348** 225
[5] Terekhin M A, Vasil'ev A N, Kamada M, Nakamura E and Kubota S 1995 *Phys. Rev.* B **52** 3117

[6] Kamenskikh I A, Munro I H, MacDonald M A, Makhov V N and Terekhin M A 1992 Synchrotron radiation *Appendix to the Daresbury Annual Report* 1991/92, p 36
[7] Pedrini C, Moine B, Bouttet D, Belsky A N, Mikhailin V V, Vasil'ev A N and Zinin E I 1993 *Chem. Phys. Lett.* **206** 470
[8] Belsky A N, Mikhailin V, Rogalev A and Zinin E I 1995 *Proc. Mater. Res. Soc. Symp.* **348** 235
[9] Ritchie R H, Tung C J, Anderson V E and Ashley J C 1975 *Radiat. Res.* **64** 181
[10] Dexter D L 1953 *J. Chem. Phys.* **21** 836
[11] Visser R, Dorenbos P, van Eijk C W E, Meijerink A, Blasse G and Hartog H W 1993 *J. Phys.: Condens. Matter* **5** 1659
[12] Ackermann Ch, Brodmann R, Hahn U, Suzuki A and Zimmerer G 1976 *Phys. Status Solidi* b **74** 579
[13] Cernik R J 1994 Synchrotron radiation *Appendix to the Daresbury Annual Report* 1993/1994, p 265
[14] Munro I H and Sabersky A P 1980 *Synchrotron Radiation Research* ed H Winick and S Doniach (New York: Plenum) p 323
[15] Gregory C M, Hayes M A, Jones G R and Pantos E 1994 *Daresbury Laboratory Technical Memorandum* DL/SCI/TM98E
[16] Anderson D F 1990 *Nucl. Instrum. Methods* A **287** 606
[17] Belsky A N, Kamenskikh I A, MacDonald M A, Makhov V N, Mikhailin V V, Munro I H, Rogalev A L, Terekhin M A and Vasil'ev A N 1992 *10th Int. Conf., VUV 10 (Paris)* abstracts, Tu 37
[18] Pedrini C, Moine B, Gacon J C and Jacquier B 1992 *J. Phys.: Condens. Mater* **4** 5461
[19] Nikl M, Mares J A, Mihokova E, Beitlerova A, Blazek K and Jindra J 1993 *Solid State Commun.* **84** 185
[20] Nikl M and Pedrini C 1994 *Solid State Commun.* **90** 155
[21] Wojtowicz A J, Balcerzyk M, Berman E and Lempicki A 1994 *Phys. Rev.* B **49** 14 880
[22] Moses W W, Derenzo S E, Weber M J, Ray-Chaudhuri A K and Cerrina F 1994 *J. Lumin.* **59** 89
[23] Elias L R, Heaps W S and Yen W M 1973 *Phys. Rev.* B **8** 4989
[24] Aleksandrov Yu M, Makhov V N and Yakimenko M N 1987 *Sov. Phys.–Solid State* **29** 1902
[25] Loh E 1967 *Phys. Rev.* **154** 270
[26] Olson C G, Piacentini M and Lynch D W 1978 *Phys. Rev.* B **18** 5740
[27] Melchakov E N, Rodnyi P A and Terekhin M A 1990 *Opt. Spectrosk.* **69** 1069